Field-of-View Constrained Impact Time Control Guidance via Time-Varying Sliding Mode Control

Shuai Ma [ID], Xugang Wang * and Zhongyuan Wang

School of Energy and Power Engineering, Nanjing University of Science and Technology, Nanjing 210094, China; ms931102@163.com (S.M.); zywnust1958@163.com (Z.W.)
* Correspondence: wxgnets@163.com

Abstract: The problem of impact time control guidance with field-of-view constraint is addressed based on time-varying sliding mode control. The kinematic conditions that satisfy the impact time control with field-of-view constraint are defined, and then a novel time-varying sliding surface is constructed to achieve the defined conditions. The sliding surface contains two unknown coefficients: one is tuned to achieve the global sliding surface to satisfy the impact time constraint and zero miss distance, and the other is tuned to guarantee the field-of-view constraint. The guidance law is designed to ensure the realization of the global sliding mode. On this basis, the guidance law is modified to a closed-loop structure, and the maximum detection capability of the seeker is utilized to a greater extent. Under the proposed guidance law, neither the small angle assumption nor time-to-go estimation is needed. The guidance command is continuous and converges to 0 at the desired impact time. Simulation results demonstrate the effectiveness and superiority of the proposed guidance law.

1. Introduction

With the development of modern defense systems, single missile penetration is increasingly difficult. As a feasible and cost-effective combat strategy, multiple missile salvo attacks have attracted wide attention in recent years [1–5]. To ensure that multiple missiles intercept targets at the same time, the missile impact time control problem needs to be considered.

In [1], an impact time control guidance (ITCG) law is derived based on linearized formulation and optimal control theory. This guidance law is a combination of the proportional navigation guidance (PNG) law and the feedback of impact time error. As an extension of [1], the authors of [6] designed a generalized ITCG law based on nonlinear formulation. The ITCG law does not need the small angle assumption and can deal with the situation of a large heading error. In [7,8], the problem of impact time control is solved by the sliding mode control technique, and the impact angle constraint is also considered in [8]. It is worth noting that the above four methods require time-to-go estimation. It is the inevitable estimation error that affects the accuracy of the designed ITCG laws. Therefore, it is necessary to design an ITCG law without time-to-go estimation. In [9], the guidance procedure is divided into two stages. In the first stage, the missile intercepts the virtual target in a limited time with a specified impact angle, and in the second stage, the missile follows the collision path until interception. To apply this guidance law, many numerical calculations are needed to determine the virtual target. In [10], the problem of impact time and angle control is also solved by sliding mode control. Different from [8], the authors construct a sliding surface to guarantee impact time control while avoiding time-to-go calculation. The authors of [11] designed an impact time and angle control guidance (ITACG) law for a moving target based on the look angle shaping technique.

The ITCG laws mentioned above can realize impact time control, but the limitation of the seeker's field-of-view (FOV) is not considered. In actual combat situations, to adjust the impact time, the missile trajectory may become highly curved. Therefore, the seeker may not be able to guarantee target locking, and the missile cannot intercept the target. Therefore, it is necessary to consider the ITCG law with FOV constraints. The authors of [12] adopted the structure of the biased proportional navigation guidance (BPNG) law to design the ITCG law. The biased term contains the cosine of the weighted lead angle to ensure the FOV constraint. As an extension of [12], the authors of [13] designed an ITCG law of a BPNG structure considering the FOV constraint and uncertain system lag. In [14], an ITACG law with FOV constraint is presented. This guidance law consists of two terms: one is used to achieve zero miss distance and impact angle constraints, and the other is used to achieve impact time constraint. The FOV constraint is guaranteed by the varying-gain approach. Different from [14], an ITACG law with FOV constraint is derived based on the look angle shaping technique in [15]. In [16], the authors consider the three-dimensional impact time control problem. Through optimal control theory, an ITCG law with FOV constraint in three-dimensional space is obtained. Although [12–16] consider the FOV constraint, they require a small angle assumption and time-to-go estimation, which is not what we want. In [17], a PNG law with time-varying navigation gain is presented. Through the time-varying navigation gain, the impact time control with FOV constraint is realized. Under this guidance law, the seeker's look angle monotonically converges to 0 from the initial value. The authors of [18] divide the guidance process into two phases. In the first phase, the lead angle remains unchanged, and in the second phase, the missile is governed by the PNG law. The time-to-go of the two phases can be calculated analytically, so the impact time can be controlled by selecting the appropriate switching point. The value of the lead angle is nonincreasing throughout the process, so the FOV constraint is not violated. In [19,20], the guidance process is also divided into two stages, and in the first stage, the lead angle remains unchanged. Different from [18], in the second stage, a new guidance law is designed to replace the PNG law, and the time-to-go of this guidance law can also be solved analytically. Therefore, the impact time can also be controlled by selecting the appropriate switching point, and the FOV constraint is not violated. The common feature of [17–20] is that the value of the lead angle does not increase throughout the process, which is why the FOV constraint is guaranteed. However, if the initial lead angle is far less than the maximum look angle of the seeker, the maximum detection capability of the seeker will not be fully utilized, which will reduce the missile's maximum achievable impact time. In [21], the desired lead angle is designed as a virtual variable that can realize impact time control with FOV constraint, and then the virtual variable is tracked by the actual lead angle based on terminal sliding mode control. However, due to the discontinuity of the derivative of the virtual variable, the guidance command will jump when the lead angle reaches the maximum. The authors of [22] use the generalized polynomial range formulation to solve the impact time control problem. To satisfy the FOV constraint, the guidance command is switched to deviated pure pursuit (DPP) when the lead angle reaches the maximum. Therefore, this method is also subject to the problem of guidance command jumps. In [23], the kinematic conditions for impact time control are defined, and then the backstepping control method is used to satisfy the defined conditions. In the backstepping control structure, the designed virtual control can realize the FOV constraint. On this basis, the achievable impact time is analyzed in [24].

Based on the above considerations, this paper focuses on the design of an ITCG law with FOV constraint. The kinematic conditions satisfying the impact time control with FOV constraint are defined, and then a time-varying sliding surface with two unknown coefficients is designed. One coefficient is tuned to achieve the global sliding surface to satisfy the zero miss distance and impact time constraint, and the other is tuned to meet the FOV constraint. The guidance law is designed to ensure the realization of the global sliding mode. Due to the open-loop structure of the proposed guidance law and the insufficient utilization of the maximum detection capability of the seeker, the guidance

law is modified to a closed-loop structure, and the maximum detection capability of the seeker is more utilized. The main advantages of the proposed ITCG law with FOV constraint are summarized as follows: First, compared with [12–16], the proposed method does not require the small angle assumption and time-to-go estimation, which avoids the degradation of guidance law performance caused by estimation error. Second, compared with [17–20], the proposed method can make more use of the seeker's maximum detection capability when the initial lead angle is far less than the maximum look angle of the seeker. Accordingly, a larger impact time can be specified for the missile. Third, compared with [21,22], under the proposed guidance law, the guidance command is continuous without jumps, which is more conducive to practical applications. Fourth, compared with [23,24], the required maximum acceleration command is significantly reduced under the proposed guidance law.

The rest of this paper is arranged as follows: In Section 2, the kinematic conditions satisfying impact time control with FOV constraint are defined. In Section 3, a novel ITCG law with FOV constraint is derived based on the time-varying sliding mode technique. The proof process and singularity analysis are also given. In Section 4, the proposed guidance law is modified to a closed-loop structure, and the seeker's maximum detection capability can be better utilized. Numerical simulations are carried out in Section 5, and the effectiveness and superiority of the proposed guidance law are verified. Finally, some conclusions are given in Section 6.

2. Problem Statement

The two-dimensional engagement geometry between the missile and stationary target in the inertial coordinate frame OXY is shown in Figure 1. M represents the missile, and T represents the stationary target. R and q represent the relative distance and line-of-sight (LOS) angle between the missile and target, respectively. V_M denotes the velocity, and a denotes the normal acceleration. The flight path angle and lead angle are denoted as θ and η, respectively.
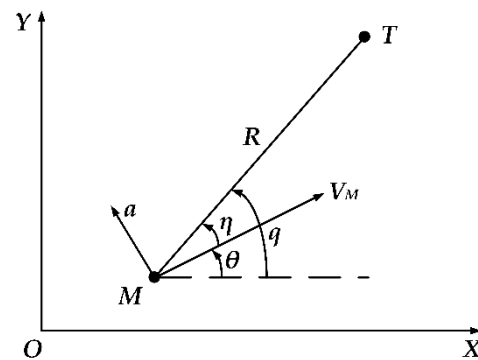
Figure 1. Planar homing engagement geometry.

The nonlinear kinematic equations between missile and target can be expressed as follows [25]:

$$\dot{R} = -V_M \cos \eta \tag{1}$$

$$R\dot{q} = V_M \sin \eta \tag{2}$$

$$\dot{\theta} = a/V_M \tag{3}$$

$$\eta = q - \theta \tag{4}$$

t_d and $\eta_{\max}$ are defined as the desired impact time and the allowable maximum lead angle, respectively. Assuming that the angle of attack is small enough to be neglected, the seeker's

FOV can be represented by the lead angle η. Therefore, the problem of impact time control guidance with FOV constraint can be expressed mathematically as

$$R(t_d) = 0, \ \eta(t_d) = 0 \tag{5}$$

$$|\eta(t)| \leq \eta_{\max} < \pi/2 \tag{6}$$

In the problem of impact time control, the calculation of time-to-go t_{go} is important. It has been mentioned that the actual value of t_{go} is difficult to obtain, and the estimation error of t_{go} will affect the accuracy of ITCG laws, so it is necessary to design an ITCG law without estimating t_{go}. Inspired by [24], if the missile follows the collision path against the target, the actual value of t_{go} can be accurately calculated as

$$t_{go} = R/V_M \tag{7}$$

If there is a time instant $t = t_f$ ($t_f < t_d$) that satisfies $\eta(t_f) = 0$ and $R(t_f) = V_M(t_d - t_f)$, the missile only needs to follow the collision path after $t = t_f$ to meet the impact time constraint. In addition, the FOV constraint in (6) should not be violated throughout the process. To implement this thought, two auxiliary states x_1 and x_2 are defined as

$$\begin{cases} x_1 = t_d - t - R/V_M \\ x_2 = -1 + \cos\eta \end{cases} \tag{8}$$

In (8), if $x_1(t_f) = 0$ and $x_2(t_f) = 0$ can be obtained, $\eta(t_f) = 0$ and $R(t_f) = V_M(t_d - t_f)$ can also be obtained, which means that impact time control and zero miss distance can be achieved. Defining $x_{2\min} = -1 + \cos\eta_{\max}$, the FOV constraint in (6) can also be converted to the constraint of x_2, which can be expressed as $x_{2\min} \leq x_2 \leq 0$. Hence, the kinematic conditions for impact time control guidance with FOV constraint can be defined as

$$\begin{cases} x_1(t_f) = 0 \\ x_2(t_f) = 0 \\ x_2(t) \geq x_{2\min} \end{cases} \tag{9}$$

In (9), the first two conditions represent the impact time constraint, and the third condition represents the FOV constraint. The dynamics of auxiliary states x_1 and x_2 can be written as

$$\begin{cases} \dot{x}_1 = x_2 \\ \dot{x}_2 = -V_M \sin^2 \eta / R + a \sin \eta / V_M \end{cases} \tag{10}$$

Hence, system (10) needs to be analyzed, and guidance command a needs to be designed to meet the defined kinematic conditions. These issues are addressed in the next section.

Remark 1. *Under the design strategy of this paper, the target is stationary, and the missile guidance process is divided into two stages. In the first stage, the missile is governed by the proposed guidance law, and the kinematic conditions defined in (9) are achieved. In the second stage, the missile follows the collision path against the stationary target, so, in theory, there is no need for guidance commands. To ensure terminal interception, the PNG law can be used in the second stage. The following content focuses on the guidance law design in the first stage, and the second stage will not be discussed.*

3. Time-Varying Sliding Mode Guidance Law Design

3.1. Impact Time Control Guidance Law Design

The first two conditions in (9) can be regarded as the finite time convergence problem of system (10), so the terminal sliding mode technique can be considered. However, the third condition in (9) also needs to be guaranteed. In this paper, the time-varying terminal sliding mode technique is used to solve this problem. A time-varying terminal sliding surface with two unknown coefficients is constructed. One coefficient is tuned to obtain the

global sliding surface to meet the impact time constraint and zero miss distance, and the other is tuned to meet the FOV constraint. The global sliding mode is guaranteed by the proposed ITCG law. To begin with, the time-varying terminal sliding surface is designed as

$$s = x_2 - (t - t_f)(\alpha t + \frac{c_0}{t_f})x_1^{1/2}, t \in [0, t_f]$$
$$\alpha = [12x_1^{1/2}(0) - 3c_0 t_f]/t_f^3 \tag{11}$$

Denote $x_1(0)$ and $x_2(0)$ as the initial values of x_1 and x_2, respectively. Therefore, we can get $x_1(0) = t_d - R_0/V_M$ and $x_2(0) = -1 + \cos\eta_0$, where R_0 and η_0 represent the initial values of R and η, respectively. It can be observed that the sliding surface $s = 0$ contains two independent unknown coefficients c_0 and t_f. The coefficient $\alpha \geq 0$ and can be determined by c_0 and t_f. The global sliding surface can be obtained by taking $c_0 = -x_2(0)/x_1^{1/2}(0)$. To guarantee $\alpha \geq 0$ and finite-time convergence before $t = t_d$, another coefficient t_f needs to satisfy

$$t_f < t_d, \ t_f \leq -4x_1(0)/x_2(0) \tag{12}$$

In (12), $t_f = t_d$ is not taken to facilitate the subsequent singularity analysis. In addition, the subsequent content will show that the coefficient t_f represents the time when x_1 and x_2 converge to 0. The coefficient c_0 has been determined, so there is only one adjustable coefficient t_f in the global sliding surface. The designed ITCG law is presented as follows:

$$a = \frac{V_M^2 \sin\eta}{R} - \frac{V_M}{\sin\eta}F(x_1, x_2, t) - \frac{kV_M}{\sin\eta}\text{sgn}(s)$$
$$F(x_1, x_2, t) = -x_1^{1/2}(2\alpha t + \frac{c_0}{t_f} - \alpha t_f) - \frac{1}{2}x_1^{-1/2}x_2[\alpha t^2 + (\frac{c_0}{t_f} - \alpha t_f)t - c_0] \tag{13}$$

In (13), k is an adjustable gain, and $k > 0$. The coefficient c_0 is determined, and the unknown coefficient t_f satisfies (12). Before determining the appropriate value of t_f, the following conclusions are given in the form of a theorem.

Theorem 1. *For system (10), by using the time-varying terminal sliding surface (11) and the guidance law (13), the following results can be obtained.*

(1)   *A global sliding mode is obtained, i.e., $s \equiv 0$ for $t \in [0, t_f]$.*
(2)   *The states x_1 and x_2 converge to 0 when t approaches t_f, i.e., $x_1(t_f) = 0$ and $x_2(t_f) = 0$.*

Proof of Theorem 1. Consider the following Lyapunov candidate:

$$V_1 = \frac{1}{2}s^2 \tag{14}$$

where V_1 is positive definite, and $V_1 \geq 0$. The derivative of V_1 can be calculated as

$$\dot{V}_1 = s\dot{s} = s[-V_M \sin^2\eta/R + a\sin\eta/V_M + F(x_1, x_2, t)] = -k|s| \leq 0 \tag{15}$$

The initial value of V_1 can be calculated as

$$V_1(0) = \frac{1}{2}s^2(0) = \frac{1}{2}[x_2(0) + c_0 x_1^{1/2}(0)]^2 = 0 \tag{16}$$

According to (14), (15) and (16), it can be concluded that $V_1 \equiv 0$ and $s \equiv 0$. Therefore, a global sliding mode is obtained for $t \in [0, t_f]$. In addition, based on (11) and $s \equiv 0$, the analytic solutions of x_1 and x_2 can be derived as follows:

$$x_1(t) = \frac{1}{36}\alpha^2 t^6 - \frac{1}{12}(\alpha^2 t_f - \frac{c_0\alpha}{t_f})t^5 + [\frac{1}{16}(\alpha t_f - \frac{c_0}{t_f})^2 - \frac{c_0\alpha}{6}]t^4 + [\frac{\alpha}{3}x_1^{1/2}(0) + \frac{c_0}{4}(\alpha t_f - \frac{c_0}{t_f})]t^3$$
$$+ [\frac{1}{4}c_0^2 - \frac{1}{2}(\alpha t_f - \frac{c_0}{t_f})x_1^{1/2}(0)]t^2 - c_0 x_1^{1/2}(0)t + x_1(0) \tag{17}$$

$$x_2(t) = \tfrac{1}{6}\alpha^2 t^5 - \tfrac{5}{12}(\alpha^2 t_f - \tfrac{c_0\alpha}{t_f})t^4 + [\tfrac{1}{4}(\alpha t_f - \tfrac{c_0}{t_f})^2 - \tfrac{2c_0\alpha}{3}]t^3 + [\alpha x_1^{1/2}(0) + \tfrac{3c_0}{4}(\alpha t_f - \tfrac{c_0}{t_f})]t^2$$
$$+ [\tfrac{1}{2}c_0^2 - (\alpha t_f - \tfrac{c_0}{t_f})x_1^{1/2}(0)]t - c_0 x_1^{1/2}(0) \tag{18}$$

Substituting $t = t_f$ into (17) and (18), it can be verified that $x_1(t_f) = 0$ and $x_2(t_f) = 0$. The verification process is a bit cumbersome. Through $s \equiv 0$, we can also get $x_1^{1/2}(t)$ and $0.5x_1^{-1/2}x_2$, which contain the third power and the second power of t, respectively. In this way, $x_1(t_f) = 0$ and $x_2(t_f) = 0$ can also be verified, and the amount of calculation can be reduced. This completes the proof. □

In Theorem 1, it has been proven that $x_1(t_f) = 0$ and $x_2(t_f) = 0$, so the first two conditions of (9) are achieved. Therefore, impact time control and zero miss distance can be achieved under guidance law (13) and global sliding surface (11).

The expression of $F(x_1, x_2, t)$ in (13) contains x_1 and x_2, so we can substitute (17) and (18) into (13). Note that (17) and (18) are derived based on $s \equiv 0$. That is, if $s \equiv 0$ cannot be maintained due to external disturbances or input saturation, (17) and (18) are invalid. Therefore, another expression of guidance law (13) for $s \equiv 0$ can be obtained as follows:

$$a = \frac{V_M^2 \sin\eta}{R} - \frac{V_M}{\sin\eta}F(t)$$
$$F(t) = -\tfrac{5}{6}\alpha^2 t^4 + \tfrac{5}{3}(\alpha^2 t_f - \tfrac{c_0\alpha}{t_f})t^3 + (\tfrac{7}{2}c_0\alpha - \tfrac{3}{4}\alpha^2 t_f^2 - \tfrac{3}{4}\tfrac{c_0^2}{t_f^2})t^2 + [\tfrac{3}{2}\tfrac{c_0^2}{t_f} - \tfrac{3}{2}c_0\alpha t_f - 2\alpha x_1^{1/2}(0)]t + (\alpha t_f - \tfrac{c_0}{t_f})x_1^{1/2}(0) - \tfrac{1}{2}c_0^2 \tag{19}$$

Compared with (19), (13) can ensure that s converges to 0 if it deviates from 0. The analytic solutions of x_1 and x_2 are still needed in subsequent FOV constraint consideration. Furthermore, it can be observed that the guidance law (13) contains time-dependent terms, so it is not a closed-loop guidance law. In Section 4, the open-loop guidance law is modified to a closed-loop structure, and the maximum detection capability of the seeker is utilized to a greater extent.

Based on the analytic solutions of x_1 and x_2, the analytic solutions of R, η and a can also be obtained. From (8), the analytic expressions of R and η represented by x_1 and x_2 can be derived as

$$R = V_M(t_d - t - x_1) \tag{20}$$

$$\eta = \text{sign}(\eta_0)\arccos(x_2 + 1) \tag{21}$$

In (21), $\text{sign}(\eta_0)$ denotes the sign function of the initial lead angle η_0. Substituting (20) and (21) into (19), the analytic solution of guidance command a can also be obtained. Therefore, without time-consuming numerical simulation, the variation of R, η and a with respect to t can be directly obtained, which is convenient for preliminary analysis and simplifies the design process.

Remark 2. *The desired impact time t_d should be larger than $R(0)/V_M$, so $x_1(0) > 0$. In addition, $x_2(0) \leq 0$. Therefore, as long as the initial lead angle is not 0, the coefficient t_f that satisfies (12) exists. It should be noted that the method proposed in this paper needs to avoid the initial lead angle being 0, and there is also an explanation of this issue in the singularity analysis.*

3.2. FOV Constraint Consideration

Impact time control can be realized by guidance law (13). Note that (13) still contains an adjustable coefficient t_f, and t_f not only can affect the convergence time of x_1 and x_2 but also can affect the maximum values of x_2 and η. In this subsection, the influence of t_f on the extreme value of x_2 is analyzed, and then the range of t_f that satisfies the FOV constraint is determined. Considering the third condition in (9), to guarantee $x_2(t) \geq x_{2\min}$, it is necessary to analyze the extreme value of x_2. The derivative of x_2 is given by

$$\dot{x}_2(t) = \tfrac{5}{6}\alpha^2 t^4 - \tfrac{5}{3}(\alpha^2 t_f - \tfrac{c_0\alpha}{t_f})t^3 + [\tfrac{3}{4}(\alpha t_f - \tfrac{c_0}{t_f})^2 - 2c_0\alpha]t^2 + [2\alpha x_1^{1/2}(0) + \tfrac{3c_0}{2}(\alpha t_f - \tfrac{c_0}{t_f})]t + \tfrac{1}{2}c_0^2 - (\alpha t_f - \tfrac{c_0}{t_f})x_1^{1/2}(0) \tag{22}$$

In (22), it can be seen that the derivative of x_2 contains the fourth power of t, so directly solving the extreme value of x_2 is complicated. After some algebraic operations, (22) can be rearranged as

$$\dot{x}_2(t) = \frac{5}{6}(t - t_f)^2 P(t)$$
$$P(t) = \alpha^2 t^2 + \frac{2c_0}{t_f}\alpha t + \frac{9}{10}\frac{c_0^2}{t_f^2} - \frac{1}{10}\alpha^2 t_f^2 - \frac{1}{5}c_0\alpha \tag{23}$$

In (23), if $\alpha = 0$, it can be verified that $\dot{x}_2 \geq 0$. To guarantee $x_2(t) \geq x_{2\min}$, $x_2(0) \geq x_{2\min}$ should be satisfied. If $\alpha > 0$, the four roots of $\dot{x}_2(t) = 0$ are denoted as t_1, t_2, t_3 and t_4, respectively, and $t_1 = t_2 = t_f$. The other two roots, t_3 and t_4, are also the roots of equation $P(t) = 0$. Δ represents the discriminant of $P(t) = 0$, which can be solved as follows:

$$\Delta = \frac{4c_0^2\alpha^2}{t_f^2} - 4\left(\frac{9}{10}\frac{c_0^2\alpha^2}{t_f^2} - \frac{1}{10}\alpha^4 t_f^2 - \frac{1}{5}c_0\alpha^3\right) = \frac{2}{5}\alpha^2\left(\frac{c_0}{t_f} + \alpha t_f\right)^2 > 0 \tag{24}$$

According to (24), t_3 and t_4 are two unequal real roots and can be analytically calculated as

$$t_3 = -\frac{c_0}{\alpha t_f} - \frac{1}{\sqrt{10}}\left(\frac{c_0}{\alpha t_f} + t_f\right)$$
$$t_4 = -\frac{c_0}{\alpha t_f} + \frac{1}{\sqrt{10}}\left(\frac{c_0}{\alpha t_f} + t_f\right) \tag{25}$$

It can be verified that $t_3 < 0$ and $t_4 < t_f$. Combining $t_1 = t_2 = t_f$, we can conclude that only t_4 needs to be analyzed for its impact on the minimum value of x_2. To simplify the subsequent discussion, define $t_{f0} = -(2\sqrt{10} - 4)x_1(0)/x_2(0)$, and the discussion can be divided into two cases:

(1) $t_f \geq t_{f0}$. It can be verified that $t_4 \leq 0$ and $\dot{x}_2(t) \geq 0$ for $t \in [0, t_f]$. Hence, x_2 increases monotonically, and the minimum value of x_2 is $x_2(0)$. To meet the FOV constraint, $x_2(0) \geq x_{2\min}$ should be satisfied.

(2) $t_f < t_{f0}$. In this case, $t_4 \in (0, t_f)$. It can be obtained that $\dot{x}_2(t) < 0$ for $t \in [0, t_4)$, and $\dot{x}_2(t) \geq 0$ for $t \in [t_4, t_f]$. Hence, to meet the FOV constraint, $x_2(t_4) \geq x_{2\min}$ should be satisfied. The value of $x_2(t_4)$ can be calculated as follows:

$$x_2(t_4) = \frac{50 - 68\sqrt{10}}{10125} \frac{\left[6x_1^{1/2}(0) - c_0 t_f\right]^5}{\left[4x_1^{1/2}(0) - c_0 t_f\right]^3 t_f} \tag{26}$$

Based on the above discussion, we can conclude that for $t_f \geq t_{f0}$ we need to ensure $x_2(0) \geq x_{2\min}$—that is, $|\eta_0| \leq \eta_{\max}$; for $t_f < t_{f0}$, $x_2(t_4) \geq x_{2\min}$ should be ensured. It can be observed that $x_2(t_4)$ completely depends on the coefficient t_f, and the FOV constraint can be satisfied by adjusting t_f. Therefore, the range of t_f satisfying the FOV constraint can be determined. For convenience, define function $Q(t_f)$, and $Q(t_f) = x_2(t_4)$. The derivative of $Q(t_f)$ with respect to t_f can be calculated as

$$\frac{dQ(t_f)}{dt_f} = \frac{50 - 68\sqrt{10}}{10125}c_0^2\frac{\left[6x_1^{1/2}(0) - c_0 t_f\right]^4}{\left[4x_1^{1/2}(0) - c_0 t_f\right]^4 t_f^2}\left[t_f^2 + \frac{8x_1(0)}{-x_2(0)}t_f - \frac{24x_1^2(0)}{x_2^2(0)}\right]$$
$$= \frac{50 - 68\sqrt{10}}{10125}c_0^2\frac{\left[6x_1^{1/2}(0) - c_0 t_f\right]^4}{\left[4x_1^{1/2}(0) - c_0 t_f\right]^4 t_f^2}(t_f - t_{f0})\left[t_f - \frac{x_1(0)}{-x_2(0)}(-2\sqrt{10} - 4)\right] \tag{27}$$

According to (12) and (27), it can be obtained that $dQ(t_f)/dt > 0$ for $t_f \in (0, t_{f0})$. In addition, it can be verified that if $t_f \to 0^+$, $Q(t_f) \to -\infty$; if $t_f \to t_{f0}$, $Q(t_f) \to x_2(0)$. Therefore, for $t_f \in (0, t_{f0})$, if $x_2(0) \geq x_{2\min}$, there must exist a constant $t_{fs} \in (0, t_{f0})$ that satisfies

$$Q(t_{fs}) = \frac{50 - 68\sqrt{10}}{10125}\frac{\left[6x_1^{1/2}(0) - c_0 t_{fs}\right]^5}{\left[4x_1^{1/2}(0) - c_0 t_{fs}\right]^3 t_{fs}} = x_{2\min} \tag{28}$$

The constant t_{fs} is the minimum value of t_f satisfying the FOV constraint. To get t_{fs}, equation (28) needs to be solved. The analytic solution of (28) is not easy to obtain, so a numerical method is considered in this paper. Thus, the allowable range of coefficient t_f satisfying the impact time with FOV constraint can be obtained as

$$t_{fs} \leq t_f < t_d, \ t_f \leq -4x_1(0)/x_2(0) \tag{29}$$

Remark 3. *The equation (28) is solved by numerical methods. Considering that $Q(t_f)$ is monotonous with respect to t_f, it is not difficult to obtain the numerical solution of t_{fs} satisfying the accuracy requirement. In addition, the numerical calculation is performed offline and will not lead to a computational burden. In this paper, the fzero function in MATLAB is used in numerical calculation.*

Remark 4. *According to (29), it can be observed that the coefficient t_f satisfying the impact time and FOV constraints is not unique. Simulation results show that the smaller the value of t_f, the faster the convergence speed of x_1 and x_2, but the larger the required guidance command and the larger the maximum value of the lead angle. Therefore, the coefficient t_f needs to be selected according to actual combat needs.*

3.3. Singularity Analysis

It has been mentioned that the guidance law (19) is another expression of (13), and it can be seen that only R and η may cause singularity. According to (8) and (29), we know that $\eta(t_f) = 0$ and $R(t_f) > 0$, so the first term of guidance law (13) does not cause singularity and only η may cause singularity. In the previous subsection, we have analyzed the monotonicity of x_2, and we find that except for $\eta(0)$ and $\eta(t_f)$, η cannot be 0 for $t \in [0, t_f]$. The singularity of the third term of guidance law (13) can also be avoided by selecting the coefficient $k = k_0 |\sin\eta|$, where k_0 is a positive constant. Hence, only the second term of guidance law (13) may cause singularity. In this subsection, we first analyze the case of $\eta(0) = 0$ and then analyze the inevitable case of $\eta(t_f) = 0$.

(1) $\eta(0) = 0$. The initial value of $F(t)$ in (13) can also be obtained by (19) and can be calculated as

$$F(0) = (\alpha t_f - \frac{c_0}{t_f})x_1^{1/2}(0) - \frac{1}{2}c_0^2 = 12x_1(0)/t_f^2 > 0 \tag{30}$$

It can be seen that the singularity occurs at $\eta(0) = 0$. Therefore, to avoid singularity, the initial lead angle cannot be 0. Remark 2 also gives a reason why the initial lead angle cannot be 0.

(2) $\eta(t_f) = 0$. According to (19), it can be verified that $F(t_f) = 0$. Taking the derivative of $F(t)$ with respect to t, we obtain

$$\dot{F}(t) = -\frac{10}{3}\alpha^2 t^3 + 5(\alpha^2 t_f - \frac{c_0\alpha}{t_f})t^2 + (7c_0\alpha - \frac{3}{2}\alpha^2 t_f^2 - \frac{3}{2}\frac{c_0^2}{t_f^2})t + \frac{3}{2}\frac{c_0^2}{t_f} - \frac{3}{2}c_0\alpha t_f - 2\alpha x_1^{1/2}(0) \tag{31}$$

According to (31), we can obtain $\dot{F}(t_f) = 0$. The guidance command $a(t_f)$ can be calculated as

$$a(t_f) = -\lim_{t \to t_f} V_M F(t) / \sin\eta(t) = \lim_{t \to t_f} \dot{F}(t) V_M^2 / a(t) \tag{32}$$

Hence, $a(t_f) = 0$ can be obtained, and no singularity occurs at $t = t_f$.

Based on the above analysis, it can be concluded that if $\eta(0) \neq 0$, no singularity problem exists, and the guidance command converges to 0 at $t = t_f$. Therefore, in order to use the guidance law (13), it is necessary to ensure that the initial lead angle is not 0. For the case where the initial lead angle is equal to 0, the flight states of the missile need to be adjusted before the guidance law (13) can be used.

4. Closed-Loop and Maximum FOV Utilization Modification

In the previous section, it was proven that the impact time control with FOV constraint can be realized through guidance law (13). However, (13) still has two obvious deficiencies in actual combat situations. First, (13) contains open-loop components. Therefore, factors such as input saturation or external disturbance may result in s not satisfying $s \equiv 0$. Although (13) can guarantee that s converges to 0, it cannot guarantee the FOV constraint when s tends to 0. Second, under guidance law (13), the maximum detection capability of the seeker is utilized less, so the maximum impact time that the missile can be specified is limited. Based on the above considerations, in this section, guidance law (13) is modified to a closed-loop structure, and the maximum detection capability of the seeker can be utilized to a greater extent.

4.1. Guidance Law Modification

It has been mentioned that guidance law (13) contains time-dependent components, i.e., open-loop components. Considering that each time instant can be regarded as the initial time, a closed-loop modification can be obtained by performing the following replacement:

$$t \rightarrow 0, x_1(0) \rightarrow x_1(t), x_2(0) \rightarrow x_2(t), c_0 \rightarrow c(t) \tag{33}$$

In (33), $c(t) = - x_2(t)/x_1^{1/2}(t)$. The modification strategy is to redesign the sliding surface and guidance law at each time instant. It can be verified that the redesigned sliding surface at each time instant is still a global sliding surface, i.e., $s \equiv 0$. The coefficient t_f and the corresponding α also need to be updated according to the current time instant as

$$\begin{aligned} t_f &\rightarrow t_f - t \\ \alpha(t) &= [12x_1^{1/2}(t) - 3c(t)(t_f - t)]/(t_f - t)^3 \end{aligned} \tag{34}$$

In (34), to guarantee $\alpha \geq 0$, $t_f - t \leq -4x_1/x_2$ should be satisfied, which will be proven in the next subsection. By substituting (33) and (34) into (13), a closed-loop guidance law is obtained as

$$\begin{aligned} a &= V_M^2 \sin \eta / R - V_M F(x_1, x_2, t) / \sin \eta \\ F(x_1, x_2, t) &= x_1^{1/2}[12x_1^{1/2} - 4c(t_f - t)]/(t_f - t)^2 - c^2/2 \end{aligned} \tag{35}$$

For convenience, t_s is defined as a time-varying coefficient, which represents the update value of coefficient t_f at each time instant. It can be found that $t_s = t_f - t$ in guidance law (35). Note that our goal is to achieve the kinematic conditions defined in (9). It does not matter whether t_s converges linearly to 0 or not, it just must be sure that $t_s \rightarrow 0$ when $t \rightarrow t_f$. Therefore, this provides the possibility for us to achieve different purposes by designing different values of t_s. Based on the above considerations, we present a general ITCG law with time-varying coefficient t_s as

$$\begin{aligned} a &= V_M^2 \sin \eta / R - V_M F(x_1, x_2, t_s) / \sin \eta \\ F(x_1, x_2, t_s) &= x_1^{1/2}(12x_1^{1/2} - 4ct_s)/t_s^2 - c^2/2 \end{aligned} \tag{36}$$

In (36), in order to ensure $\alpha \geq 0$, t_s needs to satisfy

$$0 < t_s \leq -4x_1/x_2 \tag{37}$$

In addition, if $t_s < t_f - t$, x_1 and x_2 converge faster than in the case of $t_s = t_f - t$, and vice versa. The subsequent content of this paper is to design t_s, which can increase the utilization of the maximum detection capability of the seeker while not violating the FOV constraint.

To guarantee the FOV constraint, the influence of t_s on the lead angle η should be analyzed. For convenience, define $t_{s0} = -(2\sqrt{10} - 4)x_1/x_2$ and $t_{s1} = t_f - t$. Define t_{s2} as the solution of the following equation:

$$Q_t(t_{s2}) = \frac{50 - 68\sqrt{10}}{10125} \frac{\left(6x_1^{1/2} - ct_{s2}\right)^5}{\left(4x_1^{1/2} - ct_{s2}\right)^3 t_{s2}} = x_{2\min} \tag{38}$$

It can be observed that (38) and (28) have the same structure, and t_{s2} represents the predicted minimum t_s satisfying the FOV constraint at each time instant. Equation (38) is also solved by a numerical method. The analysis results of the influence of t_s on the lead angle η are given by the following proposition.

Proposition 2. *For system (10), by using guidance law (36), the following results can be obtained.*
(1) *If $t_s \in (0, t_{s0})$, then $F(x_1, x_2, t_s) > 0$ and $|\eta|$ increases monotonically.*
(2) *If $t_s \in (t_{s0}, -4x_1/x_2]$, then $F(x_1, x_2, t_s) < 0$ and $|\eta|$ decreases monotonically.*
(3) *If $t_s = t_{s0}$, then $F(x_1, x_2, t_s) = 0$ and $\dot{\eta} = 0$.*

Proof of Proposition 2. The partial derivative of $F(x_1, x_2, t_s)$ with respect to t_s can be calculated as

$$\frac{\partial F(x_1, x_2, t_s)}{\partial t_s} = \frac{-4ct_s^2 - 2t_s(12x_1^{1/2} - 4ct_s)}{t_s^4} x_1^{1/2} = \frac{4x_1^{1/2}}{t_s^3}(ct_s - 6x_1^{1/2}) \tag{39}$$

From (39), we can get $\partial F/\partial t_s < 0$ for $t_s \in (0, -4x_1/x_2]$. Substituting $t_s = t_{s0}$ into (36), it can be obtained that

$$F(x_1, x_2, t_{s0}) = x_1^{1/2}(12x_1^{1/2} - 4ct_{s0})/t_{s0}^2 - c^2/2 = 0 \tag{40}$$

According to (39) and (40), if $t_s \in (0, t_{s0})$, $F(x_1, x_2, t_s) > 0$; if $t_s \in (t_{s0}, -4x_1/x_2]$, $F(x_1, x_2, t_s) < 0$. The derivative of the lead angle η can be obtained by (4) and (36) as

$$\dot{\eta} = \dot{q} - a/V_M = F(x_1, x_2, t)/\sin\eta \tag{41}$$

Hence, if $F(x_1, x_2, t_s) > 0$, $|\eta|$ increases monotonically; if $F(x_1, x_2, t_s) < 0$, $|\eta|$ decreases monotonically; if $F(x_1, x_2, t_s) = 0$, $\dot{\eta} = 0$. This completes the proof. $\square$

Define ε_s as a small positive constant and $\varepsilon = \eta_{\max} - |\eta|$. A design algorithm of t_s is presented in Algorithm 1. Note that t_s is a time-varying coefficient and that the value of t_s is determined by Algorithm 1 at each time instant. Under this algorithm, t_s is continuous with respect to t, and the guidance command is also continuous. In addition, the FOV constraint is not violated, and the maximum detection capability of the seeker is more utilized.

To illustrate the core idea of Algorithm 1, define a flight phase called Phase A. Phase A starts at $t_{s1} \geq t_{s0}$ and ends at $t = t_f$. In Phase A, the coefficient $t_s = t_{s1}$, and $|\eta|$ decreases monotonically according to Proposition 2. The core idea of Algorithm 1 is to reach Phase A before $t = t_f$. Once Phase A is reached, guidance law (36) is equal to (35), which can guarantee the impact time constraint. In addition, before Phase A, $|\eta|$ will not exceed $\eta_{\max}$, and in Phase A, $|\eta|$ decreases monotonically. Therefore, the impact time control

with FOV constraint can be obtained under Algorithm 1 and guidance law (36).

Algorithm 1. t_s generation process
1: for each time step do
2: Calculate t_{s0} and t_{s1}. If $t_{s1} \geq t_{s0}$, $t_s \leftarrow t_{s1}$, go to 6; if $t_{s1} < t_{s0}$, calculate ε, go to 3.
3: If $\varepsilon \leq \varepsilon_s$, go to 4; if $\varepsilon > \varepsilon_s$, go to 5.
4: $t_s \leftarrow t_{s0}$, go to 6.
5: Calculate t_{s2}. $t_s \leftarrow \max\{t_{s1}, t_{s2}\}$, go to 6.
6: Substitute t_s into guidance law to complete the simulation of this time step.
7: end for

Remark 5. *It should be noted that the t_s design algorithm is not unique. Algorithm 1 presented here is a feasible design scheme, and its advantage is that t_s is continuous with respect to t. Similarly, t_s can be designed from other perspectives, such as fast convergence and input saturation.*

4.2. Algorithm and Guidance Law Analysis

  In the previous subsection, the core idea of Algorithm 1 and the impact time control with FOV constraint capability are explained. In this subsection, three issues are analyzed. The first is whether Phase A can be reached, the second is whether coefficient t_s is continuous, and the third is whether constraint (37) can be achieved. The analysis results are given in the form of the following three propositions.

Proposition 3. *For system (10), by using guidance law (36) and Algorithm 1, Phase A can always be reached under appropriate t_f and t_d.*

Proof of Proposition 3. In Algorithm 1, if $t_{s1} \geq t_{s0}$, then $t_s \leftarrow t_{s1}$. In addition, $|\eta|$ decreases monotonically according to Proposition 1. Hence, as long as $t_{s1} \geq t_{s0}$ can be achieved, the defined Phase A can be reached. Therefore, we only need to prove that for the case of $t_{s1} < t_{s0}$, $t_{s1} \geq t_{s0}$ can finally be realized under guidance law (36) and Algorithm 1. In Algorithm 1, if $t_{s1} < t_{s0}$, regardless of whether $t_s \leftarrow t_{s0}$ or $t_s \leftarrow \max\{t_{s1}, t_{s2}\}$, $t_s \leq t_{s0}$ is satisfied. Hence, $|\eta|$ is nondecreasing according to Proposition 1. Taking the derivative of t_{s1}, we can get $dt_{s1}/dt = -1$. Taking the derivative of t_{s0}, the following is obtained:

$$dt_{s0}/dt = -(2\sqrt{10} - 4)(1 + x_1\dot{\eta}\sin\eta/x_2^2) \leq -(2\sqrt{10} - 4) < -1 \tag{42}$$

  For $t_{s1} < t_{s0}$, it can be obtained that $dt_{s0}/dt < dt_{s1}/dt$. Therefore, for properly selected t_f and t_d, $t_{s1} \geq t_{s0}$ can be finally realized. That is, Phase A can be reached under guidance law (36) and Algorithm 1. This completes the proof. □

Proposition 4. *For system (10), by using guidance law (36) and Algorithm 1, the time-varying coefficient t_s is continuous with respect to t.*

Proof of Proposition 4. Under guidance law (36) and Algorithm 1, the change in the lead angle with respect to t can be divided into four cases. Without loss of generality, taking $\eta(0) < 0$ as an example, the relationship between η and t in four cases is shown in Figure 2. These four cases need to be analyzed separately.

(1) $t_{s1}(0) \geq t_{s0}(0)$. This case is shown in Figure 2a, and the coefficient $t_s = t_{s1} = t_f - t$ throughout the process. It can be seen that t_s is continuous with respect to t, and $|\eta|$ converges monotonically.

(2) $T_{s1}(0) < t_{s0}(0)$ and $\varepsilon(0) \leq \varepsilon_s$. This case is shown in Figure 2b. $t_{s1} = t_{s0}$ is satisfied at the time instant $t = t_1$. For $t \in [0, t_1]$, we take $t_s = t_{s0}$, and the lead angle remains unchanged. For $t \in (t_1, t_f]$, we take $t_s = t_{s1}$, and $|\eta|$ converges monotonically. It can be observed that the coefficient t_s is continuous at the switching point $t = t_1$.

(3) $t_{s1}(0) < t_{s0}(0)$, $\varepsilon(0) > \varepsilon_s$ and the value of the lead angle does not increase to $\eta_{\max}$. This case is shown in Figure 2c. For $t \in [0, t_2]$, we take $t_s = \max\{t_{s1}, t_{s2}\} < t_{s0}$, and $|\eta|$

increases monotonically. $t_{s1} = t_{s0}$ is satisfied at the time instant $t = t_2$. Note that $t_s = \max\{t_{s1}, t_{s2}\} = t_{s1}$ at $t = t_2$ because $t_{s2} < t_{s0}$. For $t \in [t_2, t_f]$, we take $t_s = t_{s1}$. It can be seen that the coefficient t_s is continuous at the switching point $t = t_2$.

(4) $t_{s1}(0) < t_{s0}(0)$, $\varepsilon(0) > \varepsilon_s$ and the value of the lead angle increases to $\eta_{\max}$. This case is shown in Figure 2d. For $t \in [0, t_3]$, we take $t_s = \max\{t_{s1}, t_{s2}\}$, and $|\eta|$ increases monotonically. $t_{s1} < t_{s0}$ and $t_{s2} \approx t_{s0}$ at the time instant $t = t_3$. For $t \in (t_3, t_4]$, we take $t_s = t_{s0}$, and the lead angle remains unchanged. $t_{s1} = t_{s0}$ is satisfied at the time instant $t = t_4$. For $t \in (t_4, t_f]$, we take $t_s = t_{s1}$, and $|\eta|$ converges monotonically. The coefficient t_s is continuous at the switching points $t = t_3$ and $t = t_4$.
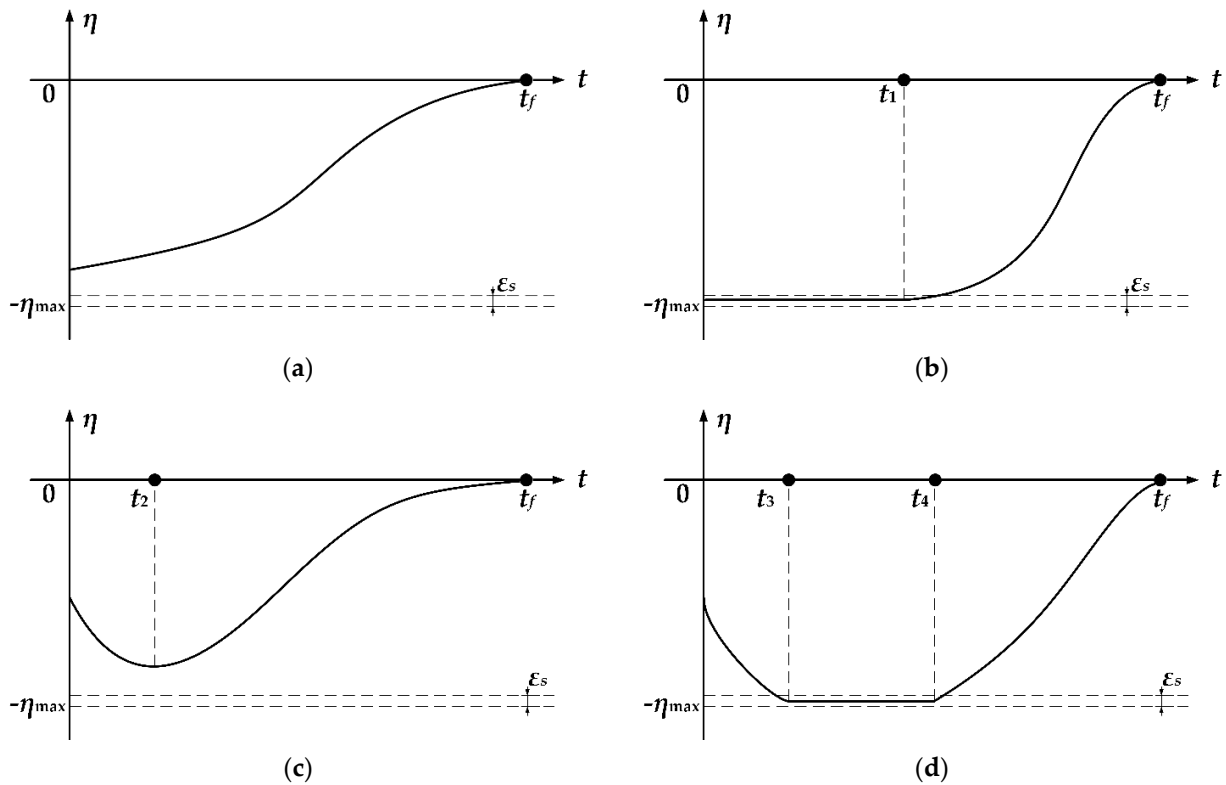

Figure 2. Four cases of lead angle with respect to t: (**a**) Variation of lead angle under case 1; (**b**) Variation of lead angle under case 2; (**c**) Variation of lead angle under case 3; (**d**) Variation of lead angle under case 4.

Based on the analysis of the above four cases, it can be concluded that t_s is continuous with respect to t under guidance law (36) and Algorithm 1. This completes the proof. □

Proposition 5. *For system (10), by using guidance law (36) and Algorithm 1, the constraint of time-varying coefficient t_s in (37) can be guaranteed.*

Proof of Proposition 5. It can be mentioned that if $t_{s1} < t_{s0}$ (before Phase A), regardless of whether $t_s \leftarrow t_{s0}$ or $t_s \leftarrow \max\{t_{s1}, t_{s2}\}$, $t_s \leq t_{s0}$ is satisfied. Therefore, $t_s \leq t_{s0} < -4x_1/x_2$ can be guaranteed before Phase A. If $t_{s1} \geq t_{s0}$ (in Phase A), $t_s \leftarrow t_{s1}$ and the guidance law is the same as (35). Hence, we should prove that $t_s = t_f - t \leq -4x_1/x_2$ under (35). For convenience, define function $H(t)$ as

$$H(t) = t_f - t + 4x_1/x_2 \tag{43}$$

The derivative of H with respect to t can be obtained as follows:

$$
\begin{aligned}
\dot{H}(t) &= -1 + 4(1 - x_1 \dot{x}_2 / x_2^2) = 3 + 4F(x_1, x_2, t) x_1 / x_2^2 \\
&= [x_2(t_f - t) + 4x_1][x_2(t_f - t) + 12x_1] / x_2^2 / (t_f - t)^2 \\
&= H(t)[x_2(t_f - t) + 12x_1] / x_2 / (t_f - t)^2
\end{aligned}
\tag{44}
$$

In (44), it can be observed that if $H < 0$, $\dot{H} > 0$; if $H = 0$, $\dot{H} = 0$. Denote the starting time of Phase A as $t = t_A$; if $t_A = 0$, we can choose $t_f \leq -4x_1(0)/x_2(0)$ to obtain $H(t_A) \leq 0$; if $t_A > 0$, it has been mentioned that Phase A begins at $t_{s1} \geq t_{s0}$, so $t_s(t_A) = t_{s1}(t_A) = t_{s0}(t_A)$ and we can obtain:

$$
H(t_A) = t_f - t_A + 4x_1(t_A)/x_2(t_A) = (8 - 2\sqrt{10})x_1(t_A)/x_2(t_A) < 0
\tag{45}
$$

According to (44) and (45), for $t \in [t_A, t_f)$, it can be seen that $H \leq 0$ in Phase A; that is, $t_s = t_f - t \leq -4x_1/x_2$ can be satisfied in Phase A. Therefore, it can be concluded that the constraint of coefficient t_s in (37) can be guaranteed. This completes the proof.　□

Remark 6. *The ITCG law in (36) finally converges to (35). When $t \to t_f$, we get $t_f - t \to 0$, $x_1(t_f) \to 0$ and $x_2(t_f) \to 0$. To avoid the adverse effect of terminal calculation error on the performance of guidance law (36), guidance law (36) is switched to PNG law when $|\eta| \leq \eta_{min}$. η_{min} is a small positive constant defined as the threshold for switching the guidance law.*

5. Simulation and Analysis

5.1. Performance Analysis of the Proposed Guidance Law

In this paper, two ITCG laws with FOV constraints are proposed: one is the open-loop guidance law (13), and the other is the modified closed-loop guidance law (36). Note that the guidance law (36) is not just a simple closed-loop modification of the guidance law (13). Compared with (13), (36) can make more use of the seeker's maximum detection capability. Obviously, the performance of the guidance law (36) is improved compared with (13). In this subsection, the effectiveness of the open-loop guidance law (13) and closed-loop guidance law (36) with Algorithm 1 is verified.

For the simulation of the guidance law (13), we want to show the influence of different convergence time t_f on the performance of the guidance law. The desired impact time is set to $t_d = 35$ s, and the specified convergence time is set to $t_f = 19.4$ s, 25 s, 30 s and 34.9 s, respectively. The input saturation is not considered. For the simulation of the guidance law (36), we want to demonstrate the performance of the guidance law under different impact time t_d. The desired impact time is set to $t_d = 30$ s, 35 s, 40 s, 45 s and 50 s, respectively. The specified convergence time is set to $t_f = t_d - 0.1$. The maximum allowable acceleration is set to $a_{max} = 5$ g, where g is the acceleration of gravity. Other necessary simulation parameters under the two guidance laws are as follows: The initial coordinates of the missile are (0, 3000) m, and the coordinates of the stationary target are (8000, 0) m. The velocity of the missile is set to $V_M = 300$ m/s, and the initial flight path angle is set to $\theta = 0°$. The maximum allowable lead angle is set to $\eta_{max} = 70°$. The threshold constants ε_s and η_{min} are set to $0.01°$ and $0.5°$, respectively. The navigation gain of PNG law is set to 3.

The simulation results of the open-loop guidance law (13) are shown in Figure 3. It can be seen from Figure 3a,b that under different values of coefficient t_f, the flight trajectory of the missile is different, but all of them can achieve target interception and impact time constraint. In addition, the flight path angle of the missile remains constant after $t = t_f$; that is, the missile flies along the collision path. Figure 3c shows the variation in the lead angle under different values of t_f. When $t_f = 19.4$ s, the maximum lead angle reaches η_{max}. Therefore, to satisfy the FOV constraint, the specified coefficient t_f cannot be less than 19.4 s. It can be verified by numerical calculation that $t_f = 19.4$ s is also the solution of (28) in this simulation scenario. The missile acceleration profile is shown in Figure 3d. It can be observed that the smaller the convergence time t_f is, the larger the required maximum

acceleration command *a*. In addition, the acceleration command *a* is continuous and converges to 0 at $t = t_f$. Therefore, the coefficient t_f has a great influence on the performance of the guidance law (13).
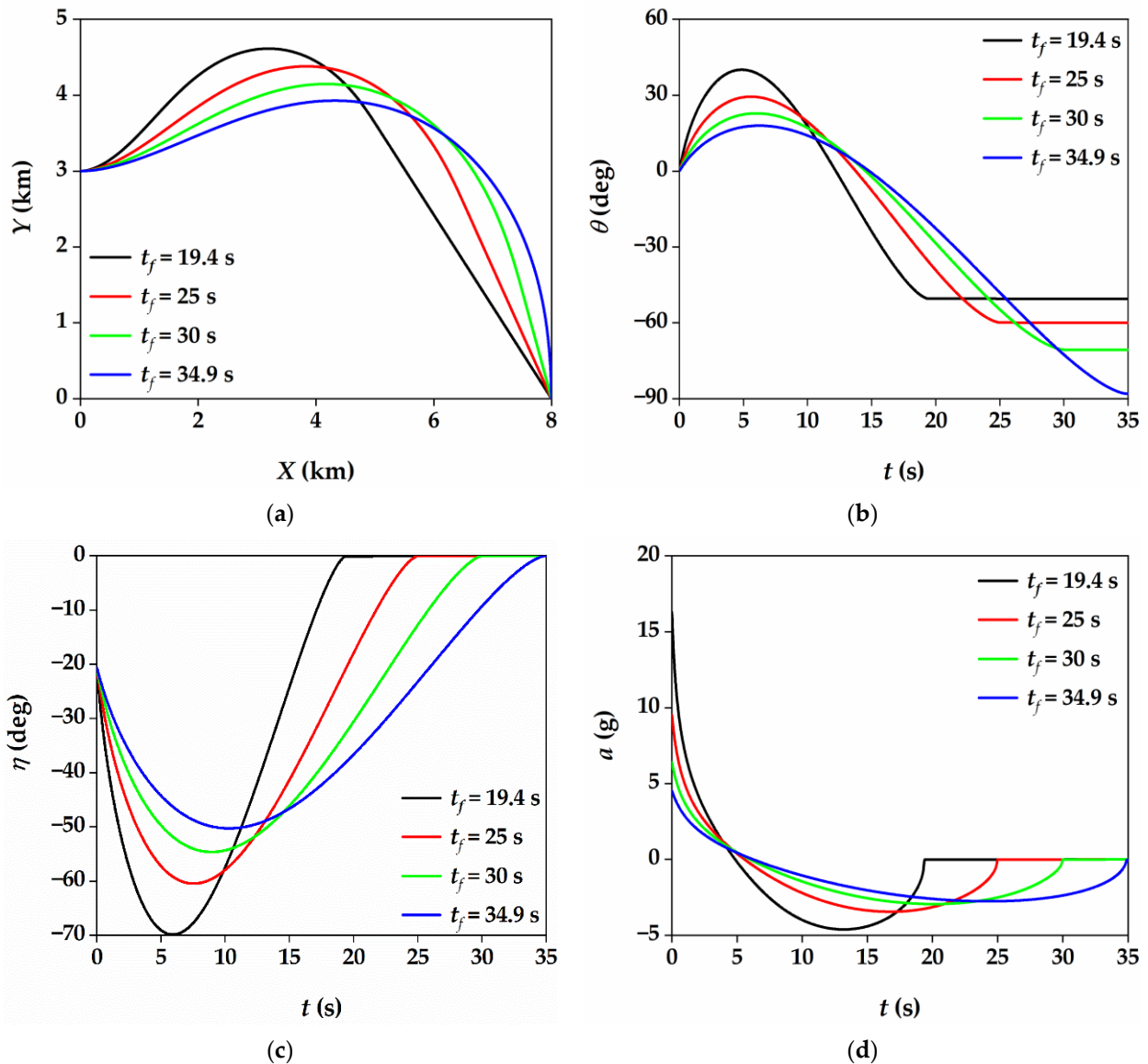

Figure 3. Simulation results of (19) under different values of coefficient t_f. (**a**) Missile flight trajectory; (**b**) Flight path angle; (**c**) Lead angle; (**d**) Missile acceleration.

The simulation results of closed-loop guidance law (36) are shown in Figure 4. The missile trajectory and the variation in flight path angle are shown in Figure 4a,b, respectively. It can be found that the missile can hit the target under different desired impact times. In addition, the longer the specified impact time, the more curved the flight trajectory and the larger the terminal flight path angle. Figure 4c shows the variation of lead angle. It can be seen that the FOV constraint of the seeker is not violated. For the cases of $t_d = 45$ s and $t_d = 50$ s, the lead angle reaches the maximum value η_{max} and remains at η_{max} for a period. The variation in coefficient t_s determined by Algorithm 1 is shown in Figure 4d. It can be seen that the change in t_s with respect to t is approximately continuous. For the cases of $t_d = 45$ s and $t_d = 50$ s, when the time t is approximately 15 s and 21 s, respectively, there is a slight jump in t_s. The slight jump is caused by the threshold parameter ε_s in Algorithm 1.

Figure 4e shows the change in the acceleration command over time, and it can also be seen that the acceleration command is continuous and finally converges to 0.
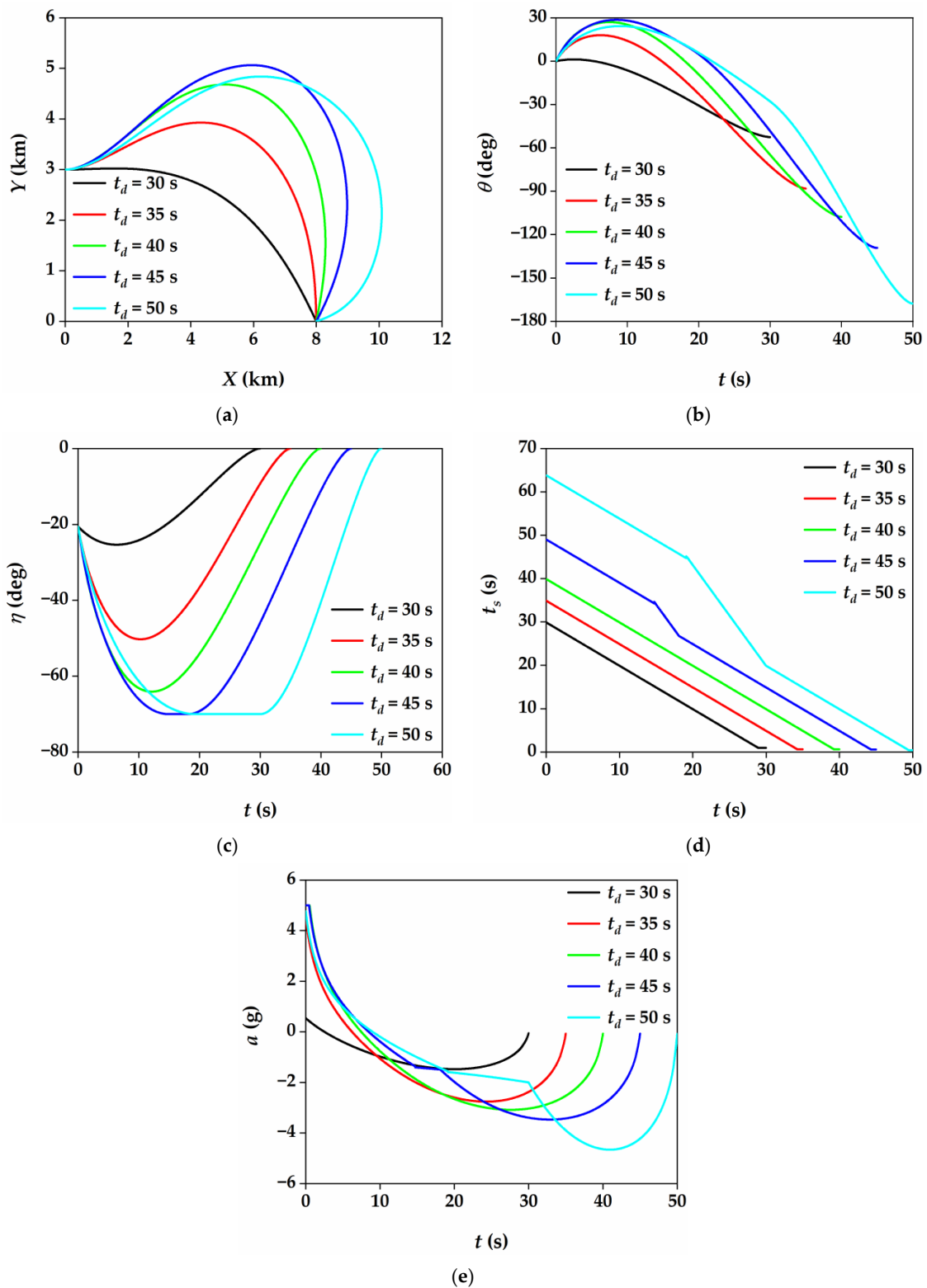

Figure 4. Simulation results of (36) under different desired impact times. (**a**) Missile flight trajectory; (**b**) Flight path angle; (**c**) Lead angle; (**d**) Profile of coefficient t_s; (**e**) Missile acceleration.

5.2. Comparative Work

The effectiveness of the proposed guidance laws is verified in Section 5.1. To verify the superiority of the proposed method, comparative work is carried out in this subsection. The ITCG law with FOV constraint proposed in [18,21,24] is selected for comparison with the closed-loop guidance law (36). The ITCG law in [18] has a simple structure and is easy to implement. The ITCG law in [21] is also designed based on the sliding mode control method. In [24], the authors' design goal is similar to that of this paper—that is, to ensure that the missile is on the collision path against the target. In this subsection, two simulation scenarios are selected to examine the performance of the above four ITCG laws. In addition, the allowable impact time range of the four guidance laws under these two scenarios is analyzed quantitatively.

The initial coordinates of the missile are (0, 0) m, and the coordinates of the stationary target are (10,000, 0) m. The velocity of the missile is set to $V_M = 250$ m/s, and the maximum lead angle is set to $\eta_{max} = 60°$. The maximum allowable acceleration is set to $a_{max} = 10$g. The desired impact time is set to $t_d = 50$ s. In scenario 1, the initial flight path angle is set to $\theta = 40°$, and the initial lead angle is less than η_{max}. In scenario 2, the initial flight path angle is set to $\theta = 60°$, and the initial lead angle is equal to η_{max}. Under the proposed guidance law (36), the values of the threshold constants and navigation gain are the same as those in Section 5.1. The coefficients required by the other three ITCG laws can be referred to [18,21,24].

The simulation results of scenario 1 are shown in Figure 5. The flight trajectory and flight path angle of the missile under the four guidance laws are shown in Figure 5a,b, respectively. Using these four guidance laws, the missile not only can intercept the target but also can ensure the impact time constraint. Compared with the methods in [18,21,24], the flight path angle changes relatively smoothly under the proposed method. Figure 5c shows the change in the lead angle η with respect to t. It can be seen that under the methods in [21,24], the value of η first increases to η_{max} and then converges to 0. The value of η is nonincreasing under the method in [18]. Under the proposed method, the value of η first increases and does not reach η_{max}, and then converges to 0. In terms of the maximum utilization of the seeker's detection capability, the method in [24] is the best, and the method in [18] is the worst. Figure 5d shows the missile acceleration under the four methods. With these four methods, the acceleration command finally converges to 0. The maximum acceleration required by the methods in [18,24] is significantly larger than that of the other two methods. The maximum acceleration required by the method in [21] is slightly larger than that under the proposed method, and the acceleration command jump occurs near $t = 12$ s. Under the proposed method, the acceleration command is continuous, and the required maximum acceleration is the smallest.
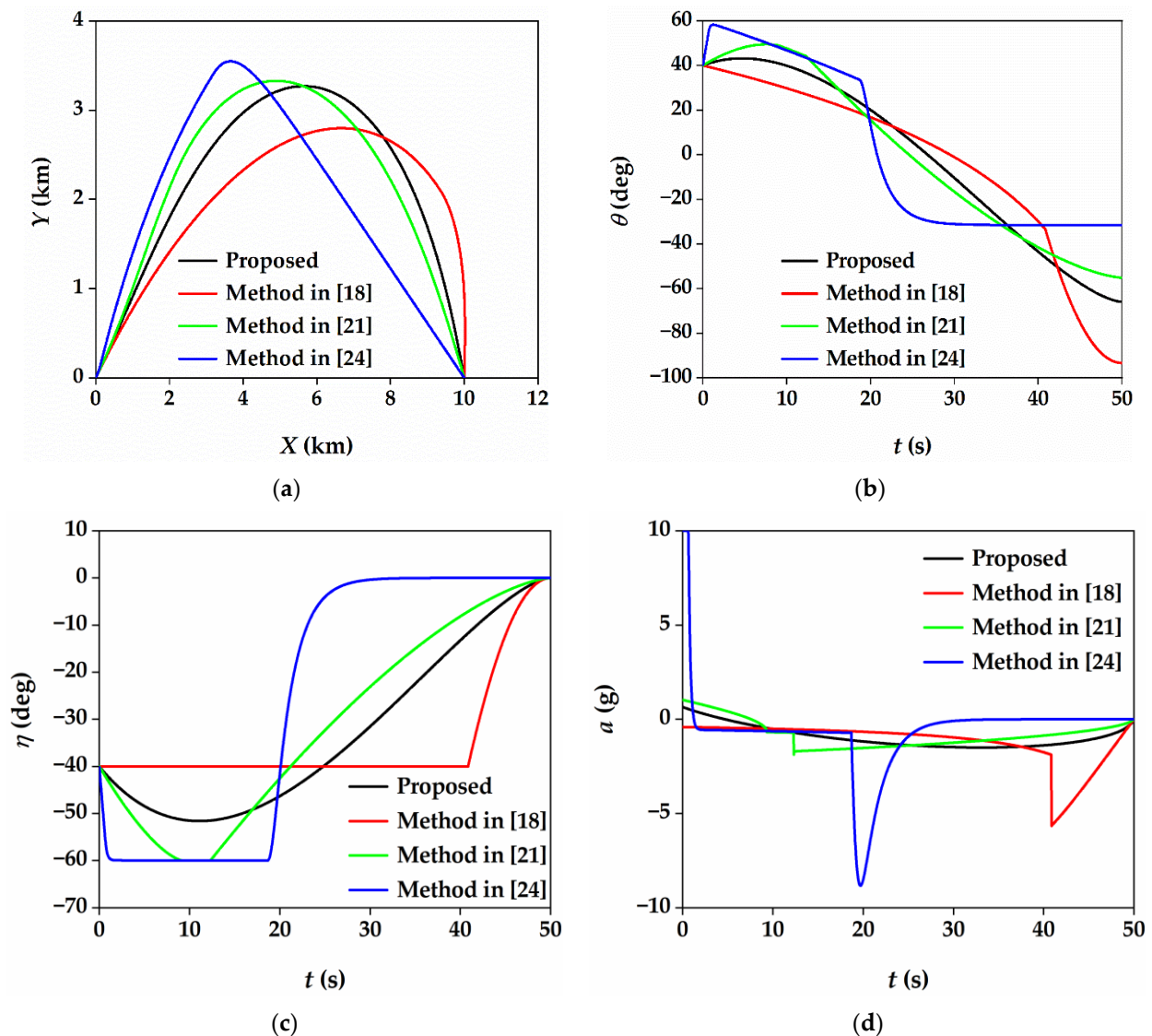
Figure 5. Simulation results of $\theta_0 = 40°$ under different guidance laws. (**a**) Missile flight trajectory; (**b**) Flight path angle; (**c**) Lead angle; (**d**) Missile acceleration.

The simulation results of scenario 2 are shown in Figure 6. Under this simulation scenario, the initial lead angle is equal to the allowable maximum lead angle, so this simulation scenario is more suitable for the method in [18] because the lead angle value is nonincreasing under the method in [18]. The simulation results are similar to those in scenario 1. A significant difference is that in scenario 2, the maximum acceleration required by the method in [18] is significantly reduced. We can see that these four methods can also achieve impact time control with FOV constraint. In addition, using the proposed method, the guidance command is continuous, and the required maximum acceleration command is the smallest.
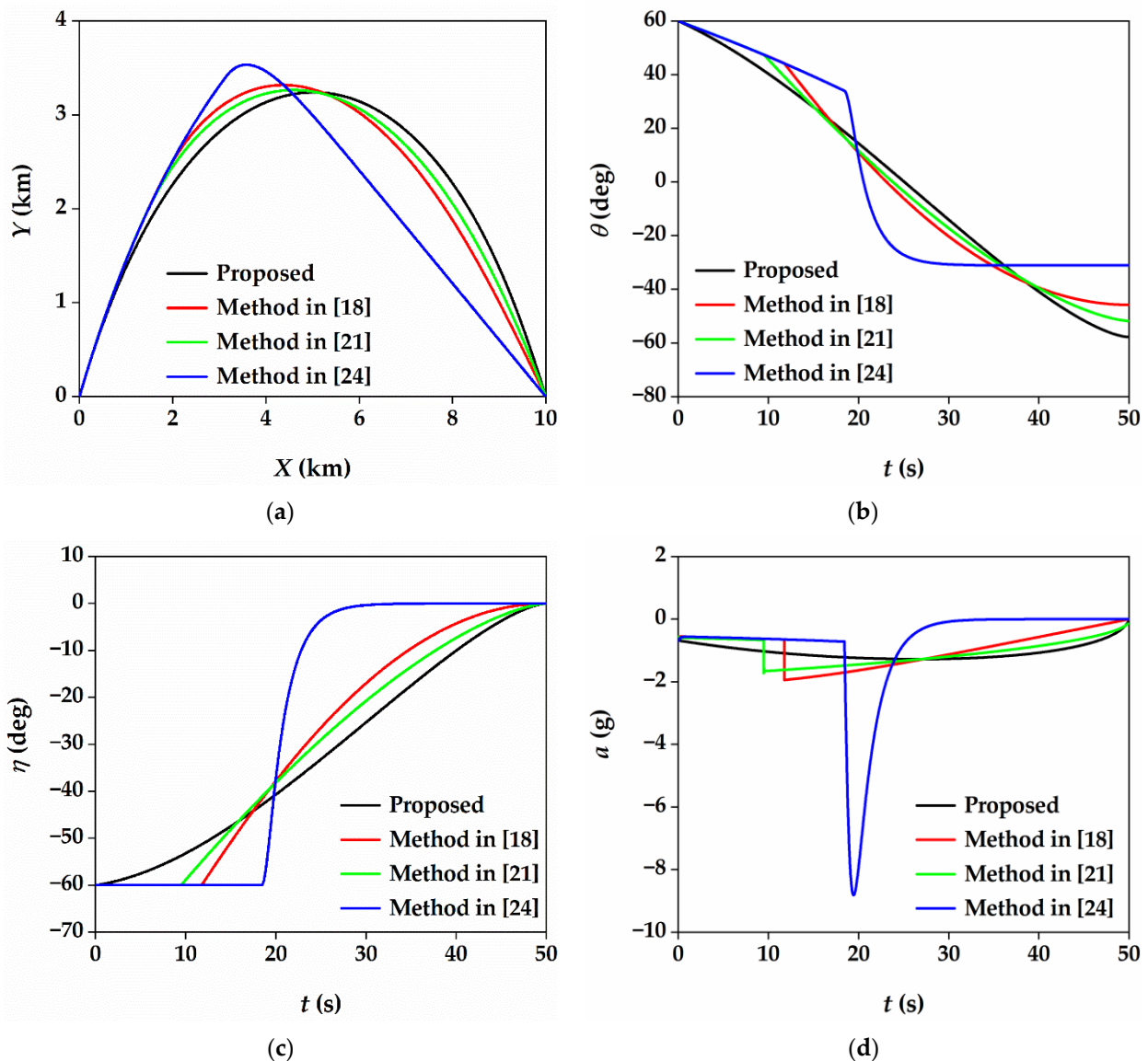
Figure 6. Simulation results of $\theta_0 = 60°$ under different guidance laws. (**a**) Missile flight trajectory; (**b**) Flight path angle; (**c**) Lead angle; (**d**) Missile acceleration.

In the aforementioned two simulation scenarios, the desired impact time is set to t_d = 50 s. Obviously, the allowable range of t_d is different under different ITCG laws. For many ITCG laws, it is difficult to give a precise allowable range of t_d through theoretical analysis. Therefore, we obtain the allowable range of t_d in the two scenarios through numerical simulation. Taking into account the actual combat scenario, it is stipulated that the allowable t_d needs to ensure that $Y \geq 0$ during the guidance process. The quantitative results are shown in Table 1. The maximum allowable impact time is denoted as $t_{d\max}$, and the minimum allowable impact time is denoted as $t_{d\min}$. It can be seen that under the method in [18], the value of $t_{d\min}$ is relatively large, and the value of $t_{d\min}$ under the other three methods has little difference. In the case of $\theta_0 = 60°$, the values of $t_{d\max}$ under the four methods are very close. In the case of $\theta_0 = 40°$, the value of $t_{d\max}$ under the method in [18] is significantly smaller than that of the other three methods. This is because the lead angle value is nonincreasing under the method in [18]. It can be seen that the value of $t_{d\max}$ is the largest under the method in [24]. The value of $t_{d\max}$ under the proposed method is 4.5 s smaller than that under the method in [24]. These results can be explained by Figure 5c,d.

Table 1. Allowable impact time range under the four ITCG laws.

	$\theta_0 = 40°$		$\theta_0 = 60°$	
	$t_{d\min}$ (s)	$t_{d\max}$ (s)	$t_{d\min}$ (s)	$t_{d\max}$ (s)
Proposed	40.4	67.4	41.1	71.2
Method in [18]	42.1	51.4	44.8	72.2
Method in [21]	40.6	69.9	41.4	71.7
Method in [24]	40.5	71.9	40.8	72.1

5.3. Salvo Attack Analysis

The scenario of a multiple missile salvo attack is simulated in this subsection. In practice, the dynamics of autopilot should be considered to examine its influence on guidance performance. We assume that all the missiles have the same autopilot, which can be modeled as a first-order transfer function as

$$\frac{a}{a_c} = \frac{1}{1 + \tau s} \tag{46}$$

where a_c is the commanded acceleration, and a is the achieved acceleration. The time constant τ is chosen as $\tau = 0.5$ s.

Consider four missiles participating in a salvo attack. The missiles are denoted as M_1, M_2, M_3 and M_4. The initial parameters of the missiles are shown in Table 2. The stationary target is located at (8000, 0) m. The allowable maximum lead angle is set to $\eta_{\max} = 60°$. The desired impact time is set to $t_d = 40$ s, and the convergence time is set to $t_f = 39.9$ s. The allowable maximum acceleration command is set to $a_{\max} = 5$ g. The threshold constants and navigation gain under the PNG law are the same as those in Section 5.2.

Table 2. Initial parameters of four missiles.

	X_0 (m)	Y_0 (m)	V_M (m/s)	θ_0 (°)
M_1	0	3000	300	0
M_2	1000	3500	280	10
M_3	1500	2800	270	20
M_4	500	3200	260	−5

The simulation results are shown in Figure 7. Figure 7a,b shows that all the missiles can hit the target at the specified impact time. The change of lead angle is shown in Figure 7c. It can be observed that the lead angles of M_1, M_2 and M_3 reach the maximum value $\eta_{\max}$ and remain for a period. None of the missiles violate the FOV constraint. The achieved acceleration commands of the missiles are shown in Figure 7d. It can be observed that the acceleration command is continuous and eventually converges to 0. Simulation results demonstrate the robustness and feasibility of the proposed guidance law, and it can be used for a salvo attack of multiple missiles.
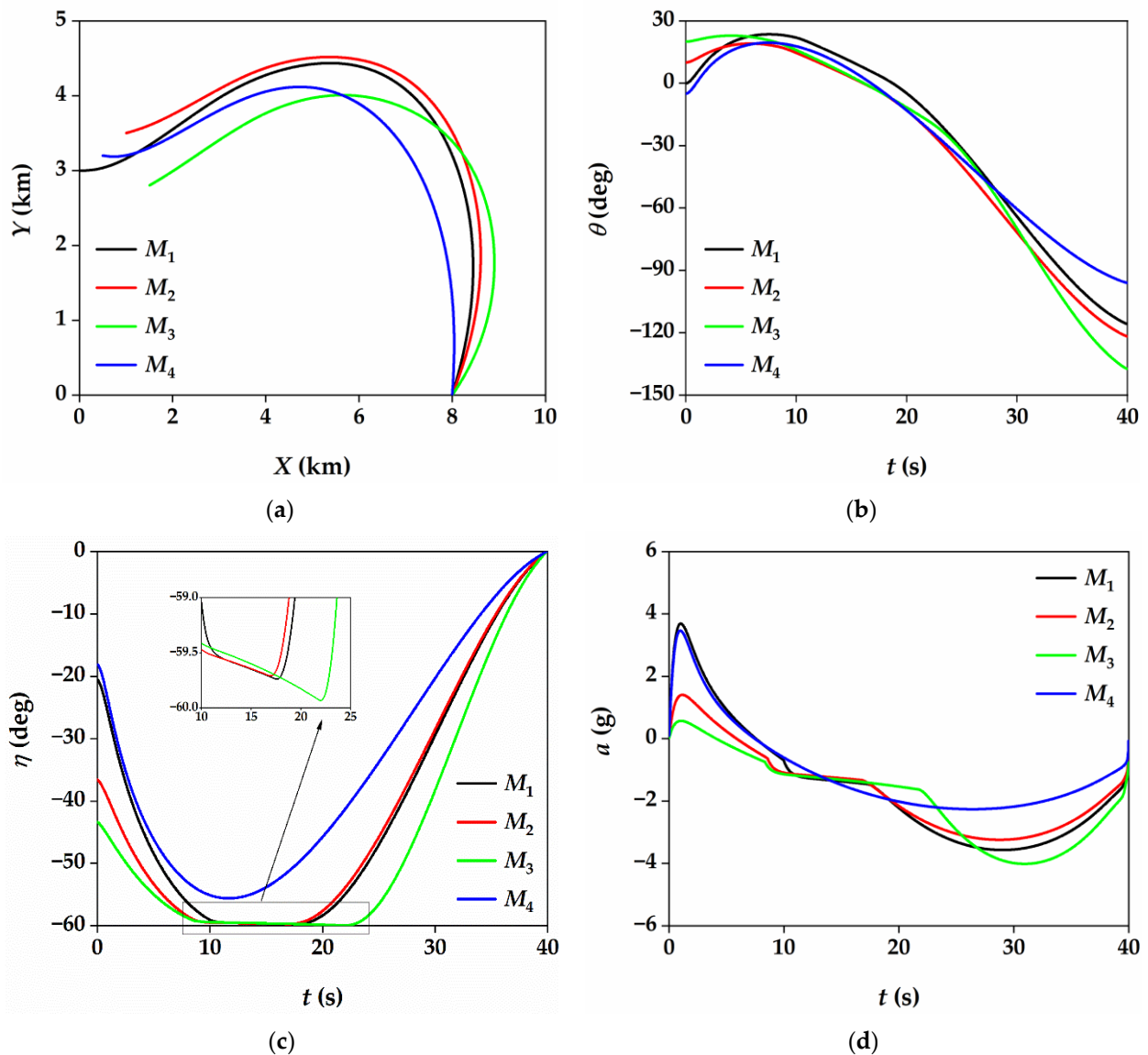
Figure 7. Simulation results of a 4 missile salvo attack. (**a**) Missile flight trajectory; (**b**) Flight path angle; (**c**) Lead angle; (**d**) Missile achieved acceleration.

6. Conclusions

A novel ITCG law with FOV constraint is derived based on the time-varying sliding mode technique. In view of the open-loop structure, the guidance law is modified to a closed-loop structure, which can make use of the seeker's maximum detection capability to a greater extent. The proposed guidance law does not require the small angle assumption or time-to-go estimation. Simulation results show that the maximum acceleration command required by the proposed guidance law is small; in addition, the acceleration command is continuous and converges to 0 at the specified time. The proposed guidance law can also be used in salvo attack scenarios. On this basis, the impact time control under velocity variation and terminal impact angle constraint will be considered in subsequent research.

Author Contributions: Conceptualization, S.M. and X.W.; methodology, S.M. and Z.W.; software, S.M.; validation, X.W. and Z.W.; writing—original draft preparation, S.M.; writing—review and editing, X.W. and Z.W.; funding acquisition, X.W. All listed authors meet the ICMJE criteria, and all who meet the four criteria are identified as authors. We attest that all authors contributed significantly to the creation of this manuscript, each having fulfilled criteria as established by the ICMJE. We

confirm that the manuscript has been read and approved by all named authors. We confirm that the order of authors listed in the manuscript has been approved by all named authors. All authors have read and agreed to the published version of the manuscript.

Institutional Review Board Statement: Not applicable.

Informed Consent Statement: Not applicable.

Data Availability Statement: The data used to support the findings of this study are available from the corresponding author upon request.

Conflicts of Interest: The authors declare that they have no conflicts of interest.

References

1. Jeon, I.S.; Lee, J.I.; Tahk, M.J. Impact-time-control guidance law for anti-ship missiles. *IEEE Trans. Control Syst. Technol.* **2006**, *14*, 260–266. [CrossRef]
2. Jeon, I.-S.; Lee, J.-I.; Tahk, M.-J. Homing Guidance Law for Cooperative Attack of Multiple Missiles. *J. Guid. Control Dyn.* **2010**, *33*, 275–280. [CrossRef]
3. Chen, Y.D.; Wang, J.A.; Shan, J.Y.; Xin, M. Cooperative Guidance for Multiple Powered Missiles with Constrained Impact and Bounded Speed. *J. Guid. Control Dyn.* **2021**, *44*, 825–841. [CrossRef]
4. Kumar, S.R.; Mukherjee, D. Terminal Time-Constrained Nonlinear Interception Strategies Against Maneuvering Targets. *J. Guid. Control Dyn.* **2021**, *44*, 200–209. [CrossRef]
5. Sinha, A.; Kumar, S.R.; Mukherjee, D. Three-Dimensional Guidance with Terminal Time Constraints for Wide Launch Envelops. *J. Guid. Control Dyn.* **2021**, *44*, 343–359. [CrossRef]
6. Jeon, I.-S.; Lee, J.-I.; Tahk, M.-J. Impact-Time-Control Guidance with Generalized Proportional Navigation Based on Nonlinear Formulation. *J. Guid. Control Dyn.* **2016**, *39*, 1885–1890. [CrossRef]
7. Cho, D.; Kim, H.J.; Tahk, M.-J. Nonsingular Sliding Mode Guidance for Impact Time Control. *J. Guid. Control Dyn.* **2016**, *39*, 61–68. [CrossRef]
8. Yang, Z.; Wang, H.; Lin, D.; Zang, L. A New Impact Time and Angle Control Guidance Law for Stationary and Nonmaneuvering Targets. *Int. J. Aerosp. Eng.* **2016**, *2016*, 1–14. [CrossRef]
9. Hu, Q.; Han, T.; Xin, M. New Impact Time and Angle Guidance Strategy via Virtual Target Approach. *J. Guid. Control Dyn.* **2018**, *41*, 1755–1765. [CrossRef]
10. Chen, X.; Wang, J. Sliding-Mode Guidance for Simultaneous Control of Impact Time and Angle. *J. Guid. Control Dyn.* **2019**, *42*, 394–401. [CrossRef]
11. Tekin, R.; Erer, K.S. Impact Time and Angle Control Against Moving Targets with Look Angle Shaping. *J. Guid. Control Dyn.* **2020**, *43*, 1020–1025. [CrossRef]
12. Zhang, Y.; Wang, X.; Wu, H. Impact time control guidance law with field of view constraint. *Aerosp. Sci. Technol.* **2014**, *39*, 361–369. [CrossRef]
13. Zhang, Y.; Wang, X.; Wu, H. Impact time control guidance with field-of-view constraint accounting for uncertain system lag. *Proc. Inst. Mech. Eng. Part G J. Aerosp. Eng.* **2015**, *230*, 515–529. [CrossRef]
14. Shim, S.-W.; Hong, S.-M.; Moon, G.-H.; Tahk, M.-J. Impact Angle and Time Control Guidance Under Field-of-View Constraints and Maneuver Limits. *Int. J. Aeronaut. Space Sci.* **2018**, *19*, 217–226. [CrossRef]
15. Kim, H.G.; Lee, J.Y.; Kim, H.J.; Kwon, H.H.; Park, J.S. Look-Angle-Shaping Guidance Law for Impact Angle and Time Control With Field-of-View Constraint. *IEEE Trans. Aerosp. Electron. Syst.* **2020**, *56*, 1602–1612. [CrossRef]
16. He, S.; Lee, C.-H.; Shin, H.-S.; Tsourdos, A. Optimal three-dimensional impact time guidance with seeker's field-of-view constraint. *Chin. J. Aeronaut.* **2021**, *34*, 240–251. [CrossRef]
17. Jeon, I.-S.; Lee, J.-I. Impact-Time-Control Guidance Law With Constraints on Seeker Look Angle. *IEEE Trans. Aerosp. Electron. Syst.* **2017**, *53*, 2621–2627. [CrossRef]
18. Lee, S.; Cho, N.; Kim, Y. Impact-Time-Control Guidance Strategy with a Composite Structure Considering the Seeker's Field-of-View Constraint. *J. Guid. Control Dyn.* **2020**, *43*, 1566–1574. [CrossRef]
19. Mukherjee, D.; Kumar, S.R. Nonlinear Impact Time Guidance with Constrained Field-of-View. In Proceedings of the 2020 American Control Conference (ACC), Denver, CO, USA, 1–3 July 2020; pp. 3802–3807.
20. Mukherjee, D.; Kumar, S.R. Field-of-View Constrained Impact Time Guidance against Stationary Targets. *IEEE Trans. Aerosp. Electron. Syst.* **2021**, in press. [CrossRef]
21. Chen, X.; Wang, J. Nonsingular Sliding-Mode Control for Field-of-View Constrained Impact Time Guidance. *J. Guid. Control Dyn.* **2018**, *41*, 1214–1222. [CrossRef]
22. Tekin, R.; Erer, K.S.; Holzapfel, F. Impact Time Control with Generalized-Polynomial Range Formulation. *J. Guid. Control Dyn.* **2018**, *41*, 1190–1195. [CrossRef]

23. Kim, H.-G.; Kim, H.J. Impact time control guidance considering seeker's field-of-view limits. In Proceedings of the 2016 IEEE 55th Conference on Decision and Control (CDC), Las Vegas, NV, USA, 12–14 December 2016; pp. 4160–4165.

24. Kim, H.-G.; Kim, H.J. Backstepping-Based Impact Time Control Guidance Law for Missiles With Reduced Seeker Field-of-View. *IEEE Trans. Aerosp. Electron. Syst.* **2019**, *55*, 82–94. [CrossRef]

25. Ha, I.-J.; Hur, J.-S.; Ko, M.-S.; Song, T.-L. Performance analysis of PNG laws for randomly maneuvering targets. *IEEE Trans. Aerosp. Electron. Syst.* **1990**, *26*, 713–721. [CrossRef]